

Very high-temperature impact melt products as evidence for cosmic airbursts and impacts 12,900 years ago

Ted E. Bunch^{a,1}, Robert E. Hermes^b, Andrew M.T. Moore^c, Douglas J. Kennett^d, James C. Weaver^e, James H. Wittke^a, Paul S. DeCarli^f, James L. Bischoff^g, Gordon C. Hillman^h, George A. Howardⁱ, David R. Kimbel^j, Gunther Kletetschka^{k,l}, Carl P. Lipo^m, Sachiko Sakaiⁿ, Zsolt Revayⁿ, Allen West^o, Richard B. Firestone^p, and James P. Kennett^q

^aGeology Program, School of Earth Science and Environmental Sustainability, Northern Arizona University, Flagstaff, AZ 86011; ^{Los Alamos National Laboratory (retired), Los Alamos, NM 87545; ^cCollege of Liberal Arts, Rochester Institute of Technology, Rochester, NY 14623; ^dDepartment of Anthropology, Pennsylvania State University, University Park, PA 16802; ^eWysys Institute for Biologically Inspired Engineering, Harvard University, Cambridge, MA 02138; ^fSRI International, Menlo Park, CA 94025; ^gUS Geological Survey, Menlo Park, CA 94025; ^hInstitute of Archaeology, University College London, London, United Kingdom; ⁱRestoration Systems, LLC, Raleigh, NC 27604; ^jKimstar Research, Fayetteville, NC 28312; ^kFaculty of Science, Charles University in Prague, and ^lInstitute of Geology, Czech Academy of Science of the Czech Republic, v.v.i., Prague, Czech Republic; ^mInstitute for Integrated Research in Materials, Environments, and Society (IIRMES), California State University, Long Beach, CA 90840; ⁿForschungsneutronenquelle Heinz Maier-Leibnitz (FRM II), Technische Universität München, Munich, Germany; ^oGeoScience Consulting, Dewey, AZ 86327; ^pLawrence Berkeley National Laboratory, Berkeley, CA 94720; and ^qDepartment of Earth Science and Marine Science Institute, University of California, Santa Barbara, CA 93106}

Edited by* Steven M. Stanley, University of Hawaii, Honolulu, HI, and approved April 30, 2012 (received for review March 19, 2012)

It has been proposed that fragments of an asteroid or comet impacted Earth, deposited silica- and iron-rich microspherules and other proxies across several continents, and triggered the Younger Dryas cooling episode 12,900 years ago. Although many independent groups have confirmed the impact evidence, the hypothesis remains controversial because some groups have failed to do so. We examined sediment sequences from 18 dated Younger Dryas boundary (YDB) sites across three continents (North America, Europe, and Asia), spanning 12,000 km around nearly one-third of the planet. All sites display abundant microspherules in the YDB with none or few above and below. In addition, three sites (Abu Hureyra, Syria; Melrose, Pennsylvania; and Blackville, South Carolina) display vesicular, high-temperature, siliceous scoria-like objects, or SLOs, that match the spherules geochemically. We compared YDB objects with melt products from a known cosmic impact (Meteor Crater, Arizona) and from the 1945 Trinity nuclear airburst in Socorro, New Mexico, and found that all of these high-energy events produced material that is geochemically and morphologically comparable, including: (i) high-temperature, rapidly quenched microspherules and SLOs; (ii) coronand, mullite, and suessite (Fe₃Si), a rare meteoritic mineral that forms under high temperatures; (iii) melted SiO₂ glass, or lechatelierite, with flow textures (or schlieren) that form at >2,200 °C; and (iv) particles with features indicative of high-energy interparticle collisions. These results are inconsistent with anthropogenic, volcanic, authigenic, and cosmic materials, yet consistent with cosmic ejecta, supporting the hypothesis of extraterrestrial airbursts/impacts 12,900 years ago. The wide geographic distribution of SLOs is consistent with multiple impactors.

tektite | microcraters | oxygen fugacity | trinitite

Manuscript Text

The discovery of anomalous materials in a thin sedimentary layer up to a few cm thick and broadly distributed across several continents led Firestone et al. (1) to propose that a cosmic impact (note that “impact” denotes a collision by a cosmic object either with Earth’s surface, producing a crater, or with its atmosphere, producing an airburst) occurred at 12.9 kiloannum (ka; all dates are in calendar or calibrated ka, unless otherwise indicated) near the onset of the Younger Dryas (YD) cooling episode. This stratum, called the YD boundary layer, or YDB, often occurs directly beneath an organic-rich layer, referred to as a black mat (2), that is distributed widely over North America and parts of South America, Europe, and Syria. Black mats also occur less frequently in quaternary deposits that are younger and older than 12.9 ka

(2). The YDB layer contains elevated abundances of iron- and silica-rich microspherules (collectively called “spherules”) that are interpreted to have originated by cosmic impact because of their unique properties, as discussed below. Other markers include sediment and magnetic grains with elevated iridium concentrations and exotic carbon forms, such as nanodiamonds, glass-like carbon, aciniform soot, fullerenes, carbon onions, and carbon spherules (3, 4). The Greenland Ice Sheet also contains high concentrations of atmospheric ammonium and nitrates at 12.9 ka, indicative of biomass burning at the YD onset and/or high-temperature, impact-related chemical synthesis (5). Although these proxies are not unique to the YDB layer, the combined assemblage is highly unusual because these YDB markers are typically present in abundances that are substantially above background, and the assemblage serves as a datum layer for the YD onset at 12.9 ka. The wide range of proxies is considered here to represent evidence for a cosmic impact that caused airbursts/impacts (the YDB event may have produced ground impacts and atmospheric airbursts) across several continents.

Since the publication of Firestone et al. (1), numerous independent researchers have undertaken to replicate the results. Two groups were unable to confirm YDB peaks in spherules (6, 7), whereas seven other groups have confirmed them (*, †, ‡,

Author contributions: T.E.B., R.E.H., A.M.M., D.J.K., J.H.W., G.K., A.W., R.B.F., and J.P.K. designed research; T.E.B., R.E.H., A.M.M., D.J.K., J.C.W., J.H.W., J.L.B., G.C.H., G.A.H., D.R.K., G.K., C.P.L., S.S., Z.R., A.W., R.B.F., and J.P.K. performed research; T.E.B., R.E.H., A.M.M., D.J.K., J.C.W., J.H.W., P.S.D., J.L.B., D.R.K., G.K., C.P.L., S.S., Z.R., A.W., R.B.F., and J.P.K. analyzed data; and T.E.B., R.E.H., A.M.M., J.H.W., P.S.D., J.L.B., A.W., R.B.F., and J.P.K. wrote the paper.

The authors declare no conflict of interest.

*This Direct Submission article had a prearranged editor.

Freely available online through the PNAS open access option.

*LeCompte MA, et al., Unusual material in early Younger Dryas age sediments and their potential relevance to the YD cosmic impact hypothesis, XVIII INQUA-Congress, July 21–27, 2011, Bern, Switzerland, paper 1813.

†Baker DW, Miranda PJ, Gibbs KE, Montana evidence for extra-terrestrial impact event that caused Ice-Age mammal die-off, American Geophysical Union, Spring Meeting, 2008, abstr P41A-05.

‡Scruggs MA, Raab LM, Murowchick JS, Stone MW, Niemi TM, Investigation of sediment containing evidence of the Younger Dryas Boundary (YDB) Impact Event, El Carrizal, Baja California Sur, Mexico, Geological Society of America Abstracts with Programs, Vol 42, no. 2, p 101 (abstr).

†To whom correspondence should be addressed. E-mail: tbeat1@cableone.net.

See Author Summary on page 11066 (volume 109, number 28).

This article contains supporting information online at www.pnas.org/lookup/suppl/doi:10.1073/pnas.1204453109/-DCSupplemental.

8–14), with most but not all agreeing that their evidence is consistent with a cosmic impact. Of these workers, Fayek et al. (8) initially observed nonspherulitic melted glass in the well-dated YDB layer at Murray Springs, Arizona, reporting “iron oxide spherules (framboids) in a glassy iron–silica matrix, which is one indicator of a possible meteorite impact.... Such a high formation temperature is only consistent with impact... conditions.” Similar materials were found in the YDB layer in Venezuela by Mahaney et al. (12), who observed “welded microspherules,... brecciated/impacted quartz and feldspar grains, fused metallic Fe and Al, and... aluminosilicate glass,” all of which are consistent with a cosmic impact.

Proxies in High-Temperature Impact Plumes. Firestone et al. (1) proposed that YDB microspherules resulted from ablation of the impactor and/or from high-temperature, impact-related melting of terrestrial target rocks. In this paper, we explore evidence for the latter possibility. Such an extraterrestrial (ET) impact event produces a turbulent impact plume or fireball cloud containing vapor, melted rock, shocked and unshocked rock debris, breccias, microspherules, and other target and impactor materials. One of the most prominent impact materials is melted siliceous glass (lechatelierite), which forms within the impact plume at temperatures of up to 2,200 °C, the boiling point of quartz. Lechatelierite cannot be produced volcanically, but can form during lightning strikes as distinctive melt products called fulgurites that typically have unique tubular morphologies (15). It is also common in cratering events, such as Meteor Crater, AZ (16), and Haughton Crater, Canada[§], as well as in probable high-temperature aerial bursts that produced melt rocks, such as Australasian tektites (17), Libyan Desert Glass (LDG) (17), Dakhleh Glass (18), and potential, but unconfirmed, melt glass from Tunguska, Siberia (19). Similar lechatelierite-rich material formed in the Trinity nuclear detonation, in which surface materials were drawn up and melted within the plume (20).

After the formation of an impact fireball, convective cells form at temperatures higher than at the surface of the sun (>4,700 °C), and materials in these cells interact during the short lifetime of the plume. Some cells will contain solidified or still-plastic impactites, whereas in other cells, the material remains molten. Some impactites are rapidly ejected from the plume to form proximal and distal ejecta depending on their mass and velocity, whereas others are drawn into the denser parts of the plume, where they may collide repeatedly, producing multiple accretionary and collisional features. Some features, such as microcraters, are unique to impacts and cosmic ablation and do not result from volcanic or anthropogenic processes[¶].

For ground impacts, such as Meteor Crater (16), most melting occurred during the formation of the crater. Some of the molten rock was ejected at high angles, subsequently interacting with the rising hot gas/particulate cloud. Most of this material ultimately fell back onto the rim as proximal ejecta, and molten material ejected at lower angles became distal ejecta. Cosmic impacts also include atmospheric impacts called airbursts, which produce some material that is similar to that produced in a ground impact. Aerial bursts differ from ground impacts in that mechanically shocked rocks are not formed, and impact markers are primarily limited to materials melted on the surface or within the plume. Glassy spherules and angular melted objects also are produced by the hot hypervelocity jet descending to the ground from the atmospheric explosion. The coupling of the airburst fireball with the upper soil layer of Earth's surface causes major melting of

material to a depth of a few cm. Svetsov and Wasson (2007)^{||} calculated that the thickness of the melted layer was a function of time and flux density, so that for $T_c > 4,700$ °C at a duration of several seconds, the thickness of melt is 1–1.5 cm. Calculations show that for higher fluxes, more soil is melted, forming thicker layers, as exemplified by Australasian tektite layered melts.

The results of an aerial detonation of an atomic bomb are similar to those of a cosmic airburst (e.g., lofting, mixing, collisions, and entrainment), although the method of heating is somewhat different because of radioactive byproducts (*SI Appendix*). The first atomic airburst occurred atop a 30-m tower at the Alamogordo Bombing Range, New Mexico, in 1945, and on detonation, the thermal blast wave melted 1–3 cm of the desert soils up to approximately 150 m in radius. The blast did not form a typical impact-type crater; instead, the shock wave excavated a shallow depression 1.4 m deep and 80 m in diameter, lifting molten and unmelted material into the rising, hot detonation plume. Other melted material was ejected at lower angles, forming distal ejecta. For Trinity, Hermes and Strickfaden (20) estimated an average plume temperature of 8,000 °C at a duration of 3 s and an energy yield of up to 18 kilotons (kt) trinitrotoluene (TNT) equivalent. Fallback of the molten material, referred to as trinitite, littered the surface for a diameter of 600 m, in some places forming green glass puddles (similar to Australasian layered tektites). The ejecta includes irregularly shaped fragments and aerodynamically shaped teardrops, beads, and dumbbell glasses, many of which show collision and accretion features resulting from interactions in the plume (similar to Australasian splash-form tektites). These results are identical to those from known cosmic airbursts. *SI Appendix, Table S1* provide a comparison of YDB objects with impact products from Meteor Crater, the Australasian tektite field, and the Trinity nuclear airburst.

Scope of Study. We investigated YDB markers at 18 dated sites, spanning 12,000 km across seven countries on three continents (*SI Appendix, Fig. S1*), greatly expanding the extent of the YDB marker field beyond earlier studies (1). Currently, there are no known limits to the field. Using both deductive and inductive approaches, we searched for and analyzed YDB spherules and melted siliceous glass, called scoria-like objects (SLOs), both referred to below as YDB objects. The YDB layer at all 18 sites contains microspherules, but SLOs were found at only three sites: Blackville, South Carolina; Abu Hureyra, Syria; and Melrose, Pennsylvania. Here, we focus primarily on abundances, morphology, and geochemistry of the YDB SLOs. Secondly, we discuss YDB microspherules with regard to their geochemical similarity and co-occurrence with SLOs. We also compare compositions of YDB objects to compositions: (i) of materials resulting from meteoritic ablation and from terrestrial processes, such as volcanism, anthropogenesis, and geological processes; and (ii) from Meteor Crater, the Trinity nuclear detonation, and four ET aerial bursts at Tunguska, Siberia; Dakhleh Oasis, Egypt; Libyan Desert Glass Field, Egypt; and the Australasian tektite strewnfield, SE Asia.

For any investigation into the origin of YDB objects, the question arises as to whether these objects formed by cosmic impact or by some other process. This is crucial, because sedimentary spherules are found throughout the geological record and can result from nonimpact processes, such as cosmic influx, meteoritic ablation, anthropogenesis, lightning, and volcanism. However, although microspherules with widely varying origins can appear superficially similar, their origins may be determined with reasonably high confidence by a combination of various analyses—e.g., scanning electron microscopy with energy dispersive spectroscopy

[§]Osinski GF, Bunch TE, Wittke J, Evidence for shock melting of carbonates from Meteor Crater, Arizona, Annual Meeting of the Meteoritical Society, July 28–August 1, 2003, abstr 5070.

[¶]Buchner E, Schmeider M, Strasser A, Krochert L, Impacts on spherules, 40th Lunar and Planetary Science Conference. March 26, 2009, abstr 1017.

^{||}Svetsov VV, Wasson JT, Melting of soil rich in quartz by radiation from aerial bursts—A possible cause of the formation for Libyan Desert Glass and layered Australasian tektites, 38th Lunar and Planetary Science Conference. March 13, 2007, abstr 1499.

(SEM-EDS) and wavelength-dispersive spectroscopy (WDS) by electron microprobe—to examine evidence for microcratering, dendritic surface patterns produced during rapid melting—quenching **, and geochemical composition. Results and discussion are below and in the *SI Appendix*.

SLOs at YDB Sites. Abu Hureyra, Syria. This is one of a few archaeological sites that record the transition from nomadic hunter—gatherers to farmer—hunters living in permanent villages (21). Occupied from the late Epipalaeolithic through the Early Neolithic (13.4–7.5 ka), the site is located close to the Euphrates River on well-developed, highly calcareous soils containing platy flint (chert) fragments, and the regional valley sides are composed of chalk with thin beds of very fine-grained flint. The dominant lithology is limestone within a few km, whereas gypsum deposits are prominent 40 km away, and basalt is found 80 km distant. Much of this part of northern Syria consists of highly calcareous Mediterranean, steppe, and desert soils. To the east of Abu Hureyra, there are desert soils marked by wind-polished flint fragments forming a pediment on top of marls (calcareous and clayey mudstones). Thus, surface sediments and rocks of the entire region are enriched in CaO and SiO₂. Moore and co-workers excavated the site in 1972 and 1973, and obtained 13 radiocarbon dates ranging from 13.37 ± 0.30 to 9.26 ± 0.13 cal ka B.P., including five that ranged from 13.04 ± 0.15 to 12.78 ± 0.14 ka, crossing the YDB interval (21) (*SI Appendix, Table S2*). Linear interpolation places the date of the YDB layer at 12.9 ± 0.2 ka (1σ probability) at a depth of 3.6 m below surface (mbs) at 284.7 m above sea level (m asl) (*SI Appendix, Figs. S2D and S3*). The location of the YDB layer is further supported by evidence of 12.9-ka climatic cooling and drying based on the palynological and macrobotanical record that reveal a sudden decline of 60–100% in the abundance of charred seed remains of several major groups of food plants from Abu Hureyra. Altogether, more than 150 species of plants showed the distinct effects of the transition from warmer, moister conditions during the Bølling-Allerød (14.5–12.9 ka) to cooler, dryer condition during the Younger Dryas (12.9–11.5 ka).

Blackville, South Carolina. This dated site is in the rim of a Carolina Bay, one of a group of >50,000 elliptical and often overlapping depressions with raised rims scattered across the Atlantic Coastal Plain from New Jersey to Alabama (*SI Appendix, Fig. S4*). For this study, samples were cored by hand auger at the thickest part of the bay rim, raised 2 m above the surrounding terrain. The sediment sequence is represented by eolian and alluvial sediments composed of variable loamy to silty red clays down to an apparent unconformity at 190 cm below surface (cmbs). Below this there is massive, variegated red clay, interpreted as a paleosol predating bay rim formation (Miocene marine clay >1 million years old) (*SI Appendix, Fig. S4*). A peak in both SLOs and spherules occurs in a 15 cm—thick interval beginning at 190 cmbs above the clay section, extending up to 175 cmbs (*SI Appendix, Table S3*). Three optically stimulated luminescence (OSL) dates were obtained at 183, 152, and 107 cmbs, and the OSL date of 12.96 ± 1.2 ka in the proxy-rich layer at 183 cmbs is consistent with Firestone et al. (1) (*SI Appendix, Fig. S4 and Table S2*).

Melrose, Pennsylvania. During the Last Glacial Maximum, the Melrose area in NE Pennsylvania lay beneath 0.5–1 km of glacial ice, which began to retreat rapidly after 18 ka (*SI Appendix, Fig. S5*). Continuous samples were taken from the surface to a depth of 48 cmbs, and the sedimentary profile consists of fine-grained, humic colluvium down to 38 cmbs, resting on sharply

defined end-Pleistocene glacial till (diamicton), containing 40 wt% angular clasts >2 mm in diameter. Major abundance peaks in SLOs and spherules were encountered above the till at a depth of 15–28 cmbs, consistent with emplacement after 18 ka. An OSL date was acquired at 28 cmbs, yielding an age of 16.4 ± 1.6 ka, and, assuming a modern age for the surface layer, linear interpolation dates the proxy-rich YDB layer at a depth of 21 cmbs to 12.9 ± 1.6 ka (*SI Appendix, Fig. S5 and Table S2*).

YDB sites lacking SLOs. The other 15 sites, displaying spherules but no SLOs, are distributed across six countries on three continents, representing a wide range of climatic regimes, biomes, depositional environments, sediment compositions, elevations (2–1,833 m), and depths to the YDB layer (13 cm–14.0 m) (*SI Appendix, Fig. S1*). YDB spherules and other proxies have been previously reported at seven of the 18 sites (1). The 12.9-ka YDB layers were dated using accelerator mass spectrometry (AMS) radiocarbon dating, OSL, and/or thermal luminescence (TL).

Results and Discussion

Impact-Related Spherules Description. The YDB layer at 18 sites displays peaks in Fe- and/or Si-rich magnetic spherules that usually appear as highly reflective, black-to-clear spheroids (Fig. 1 and *SI Appendix, Fig. S6 A–C*), although 10% display more complex shapes, including teardrops and dumbbells (*SI Appendix Fig. S6 D–H*). Spherules range from 10 μm to 5.5 mm in diameter (mean, 240 μm; median, 40 μm), and concentrations range from 5–4,900 spherules/kg (mean, 940/kg; median, 180/kg) (Fig. 2 and *SI Appendix, Table S3*). Above and below the YDB layer, concentrations are zero to low. SEM imaging reveals that the outer surfaces of most spherules exhibit distinctive skeletal (or dendritic) textures indicative of rapid quenching producing varying levels of coarseness (*SI Appendix, Fig. S7*). This texture makes them easily distinguishable from detrital magnetite, which is typically fine-grained and monocrystalline, and from framboidal grains, which are rounded aggregates of blocky crystals. It is crucial to note that these other types of grains cannot be easily differentiated from impact spherules by light microscopy and instead require investigation by SEM. Textures and morphologies of YDB spherules correspond to those observed in known impact events, such as at the 65-million-year-old Cretaceous—Paleogene boundary, the 50-ka Meteor Crater impact, and the Tunguska airburst in 1908 (*SI Appendix, Fig. S7*).

SLOs Description. Three sites contained conspicuous assemblages of both spherules and SLOs that are composed of shock-fused vesicular siliceous glass, texturally similar to volcanic scoria. Most SLOs are irregularly shaped, although frequently they are com-

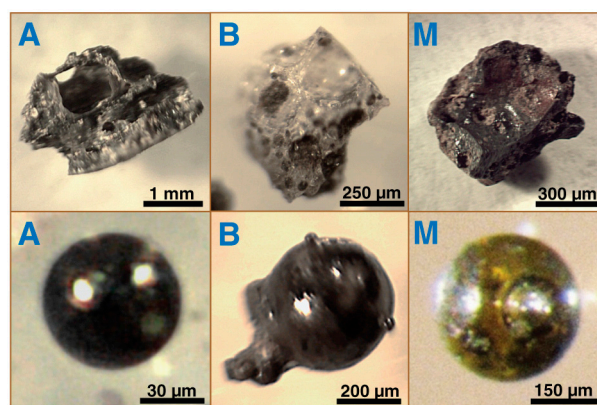


Fig. 1. Light photomicrographs of YDB objects. (Upper) SLOs and (Lower) magnetic spherules. A = Abu Hureyra, B = Blackville, M = Melrose.

**Petaev ML, Jacobsen SB, Basu AR, Becker L, Magnetic Fe,Si,Al-rich impact spherules from the P-T Boundary Layer at Graphite Peak, Antarctica, 35th Lunar and Planetary Science Conference, March 16, 2004, abstr 1216.

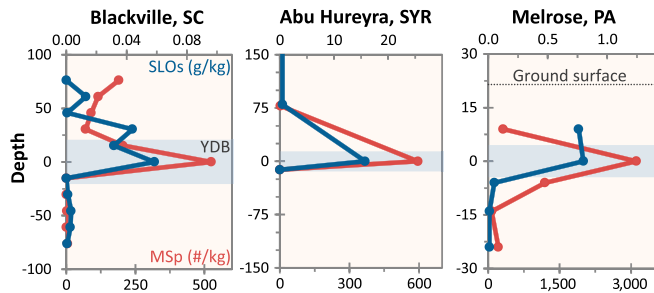


Fig. 2. Site graphs for three key sites. SLOs and microspherules exhibit significant peaks in YDB layer. Depth is relative to YDB layer, represented by the light blue bar.

posed of several fused, subrounded glassy objects. As compared to spherules, most SLOs contain higher concentrations of Si, Al, and Ca, along with lower Fe, and they rarely display the dendritic textures characteristic of most Fe-rich spherules. They are nearly identical in shape and texture to high-temperature materials from the Trinity nuclear detonation, Meteor Crater, and other impact craters (*SI Appendix, Fig. S8*). Like spherules, SLOs are generally dark brown, black, green, or white, and may be clear, translucent, or opaque. They are commonly larger than spherules, ranging from 300 μm to 5.5 mm long (mean, 1.8 mm; median, 1.4 mm) with abundances ranging from 0.06–15.76 g/kg for the magnetic fraction that is $>250 \mu\text{m}$. At the three sites, spherules and SLOs co-occur in the YDB layer dating to 12.9 ka. Concentrations are low to zero above and below the YDB layer.

Geochemistry of YDB Objects. Comparison to cosmic spherules and micrometeorites. We compared Mg, total Fe, and Al abundances for 70 SLOs and 340 spherules with >700 cosmic spherules and micrometeorites from 83 sites, mostly in Antarctica and Greenland (*Fig. 3A*). Glassy Si-rich extraterrestrial material typically exhibits MgO enrichment of $17\times$ (avg 25 wt%) (23) relative to YDB spherules and SLOs from all sites (avg 1.7 wt%), the same as YDB magnetic grains (avg 1.7 wt%). For Al_2O_3 content, extraterrestrial material is depleted $3\times$ (avg 2.7 wt%) relative to YDB spherules and SLOs from all sites (avg 9.2 wt%), as well as YDB magnetic grains (avg 9.2 wt%). These results indicate $>90\%$ of YDB objects are geochemically distinct from cosmic material.

Comparison to anthropogenic materials. We also compared the compositions of the YDB objects to >270 anthropogenic spherules and fly ash collected from 48 sites in 28 countries on five continents (*Fig. 3B* and *SI Appendix, Table S5*), primarily produced by one of the most prolific sources of atmospheric contamination: coal-fired power plants (24). The fly ash is $3\times$ enriched in Al_2O_3 (avg 25.8 wt%) relative to YDB objects and magnetic grains (avg 9.1 wt%) and depleted $2.5\times$ in P_2O_5 (0.55 vs. 1.39 wt%, respectively). The result is that 75% of YDB objects have compositions different from anthropogenic objects. Furthermore, the potential

for anthropogenic contamination is unlikely for YDB sites, because most are buried 2–14 mbs.

Comparison to volcanic glasses. We compared YDB objects with $>10,000$ volcanic samples (glass, tephra, and spherules) from 205 sites in four oceans and on four continents (*SI Appendix, Table S5*). Volcanic material is enriched $2\times$ in the alkalis, $\text{Na}_2\text{O} + \text{K}_2\text{O}$ (avg 3 wt%), compared with YDB objects (avg 1.5 wt%) and magnetic grains (avg 1.2 wt%). Also, the Fe concentrations for YDB objects (avg 55 wt%) are enriched $5.5\times$ compared to volcanic material (avg 10 wt%) (*Fig. 3C*), which tends to be silica-rich ($>40 \text{ wt}\%$) with lower Fe. Approximately 85% of YDB objects exhibit compositions dissimilar to silica-rich volcanic material. Furthermore, the YDB assemblages lack typical volcanic markers, including volcanic ash and tephra.

Melt temperatures. A $\text{FeO}^{\text{T}}\text{-Al}_2\text{O}_3\text{-SiO}_2$ phase diagram reveals three general groups of YDB objects (*Fig. 3D*). A Fe-rich group, dominated by the mineral magnetite, forms at temperatures of approximately 1,200–1,700 $^{\circ}\text{C}$. The high-Si/low-Al group is dominated by quartz, plagioclase, and orthoclase and has liquidus temperatures of 1,200–1,700 $^{\circ}\text{C}$. An Al–Si-rich group is dominated by mullite and corundum with liquidus temperatures of 1,400–2,050 $^{\circ}\text{C}$. Because YDB objects contain more than the three oxides shown, potentially including H_2O , and are not in equilibrium, the liquidus temperatures are almost certainly lower than indicated. On the other hand, in order for high-silica material to produce low-viscosity flow bands (schlieren), as observed in many SLOs, final temperatures of $>2,200 \text{ }^{\circ}\text{C}$ are probable, thus eliminating normal terrestrial processes. Additional temperatures diagrams are shown in *SI Appendix, Fig. S9*.

Comparison to impact-related materials. Geochemical compositions of YDB objects are presented in a $\text{Al}_2\text{O}_3\text{-CaO-FeO}^{\text{T}}$ ternary diagram used to plot compositional variability in metamorphic rocks (*Fig. 4A*). The diagram demonstrates that the composition of YDB objects is heterogeneous, spanning all metamorphic rock types (including pelitic, quartzofeldspathic, basic, and calcareous). From 12 craters and tektite strewnfields on six continents, we compiled compositions of $>1,000$ impact-related markers (spherules, ejecta, and tektites, which are melted glassy objects), as well as 40 samples of melted terrestrial sediments from two nuclear aerial detonations: Trinity (22) and Yucca Flat (25) (*Fig. 4B* and *SI Appendix, Table S5*). The compositions of YDB impact markers are heterogeneous, corresponding well with heterogeneous nuclear melt material and impact proxies.

Comparison to terrestrial sediments. We also used the acriflavine system to analyze $>1,000$ samples of bulk surface sediment, such as clay, mud, and shale, and a wide range of terrestrial metamorphic rocks. YDB objects (*Fig. 4A*) are similar in composition to surface sediments, such as clay, silt, and mud (25) (*Fig. 4C*),

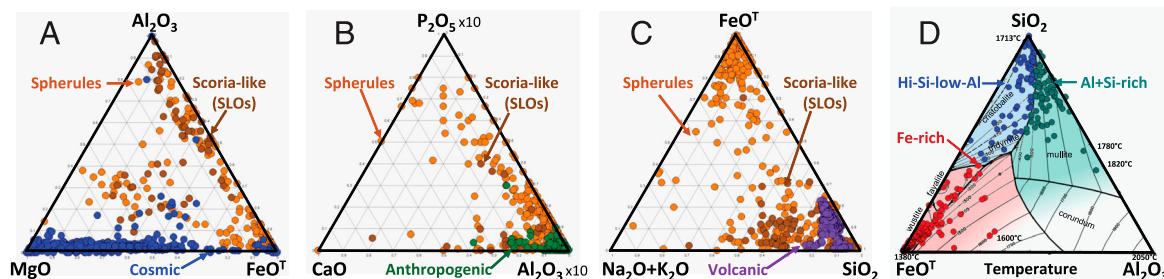


Fig. 3. Ternary diagrams comparing molar oxide wt% of YDB SLOs (dark orange) and magnetic spherules (orange) to (A) cosmic material, (B) anthropogenic material, and (C) volcanic material. (D) Inferred temperatures of YDB objects, ranging up to 1,800 $^{\circ}\text{C}$. Spherules and SLOs are compositionally similar; both are dissimilar to cosmic, anthropogenic, and volcanic materials.

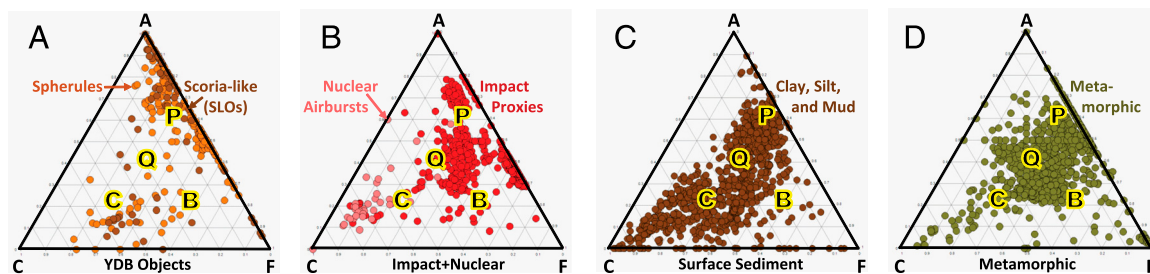


Fig. 4. Compositional ternary diagrams. (A) YDB objects: Spherules (orange) and SLOs (dark orange) are heterogeneous. Letters indicate plot areas typical of specific metamorphic rock types: P = pelitic (e.g., clayey mudstones and shales), Q = quartzofeldspathic (e.g., gneiss and schist), B = basic (e.g., amphibolite), and C = calcareous (e.g., marble) (40). (B) Cosmic impact materials in red ($N > 1,000$) with nuclear material in light red. (C) Surface sediments, such as clay, silt, and mud (41). (D) Metamorphic rocks. Formula for diagrams: $A = (Al_2O_3 + Fe_2O_3) \cdot (Na_2O + K_2O)$; $C = [CaO - (3.33 \times P_2O_5)]$; $F = (FeO + MgO + MnO)$.

and to metamorphic rocks, including mudstone, schist, and gneiss (25) (Fig. 4D).

In addition, rare earth element (REE) compositions of the YDB objects acquired by instrumental neutron activation analysis (INAA) and prompt gamma activation analysis (PGAA) are similar to bulk crust and compositions from several types of tektites, composed of melted terrestrial sediments (*SI Appendix*, Fig. S104). In contrast, REE compositions differ from those of chondritic meteorites, further confirming that YDB objects are not typical cosmic material. Furthermore, relative abundances of La, Th, and Sc confirm that the material is not meteoritic, but rather is of terrestrial origin (*SI Appendix*, Fig. S10B). Likewise, Ni and Cr concentrations in YDB objects are generally unlike those of chondrites and iron meteorites, but are an excellent match for terrestrial materials (*SI Appendix*, Fig. S10C). Overall, these results indicate SLOs and spherules are terrestrial in origin, rather than extraterrestrial, and closely match known cosmic impact material formed from terrestrial sediments.

We investigated whether SLOs formed from local or nonlocal material. Using SEM-EDS percentages of nine major oxides (97 wt%, total) for Abu Hureyra, Blackville, and Melrose, we compared SLOs to the composition of local bulk sediments, acquired with NAA and PGAA (*SI Appendix*, Table S4). The results for each site show little significant difference between SLOs and bulk sediment (*SI Appendix*, Fig. S11), consistent with the hypothesis that SLOs are melted local sediment. The results demonstrate that SLOs from Blackville and Melrose are geochemically similar, but are distinct from SLOs at Abu Hureyra, suggesting that there are at least two sources of melted terrestrial material for SLOs (i.e., two different impacts/airbursts).

We also performed comparative analyses of the YDB object dataset demonstrating that: (i) proxy composition is similar regardless of geographical location (North America vs. Europe vs. Asia); (ii) compositions are unaffected by method of analysis (SEM-EDS vs. INAA/PGAA); and (iii) compositions are comparable regardless of the method of preparation (sectioned vs. whole) (*SI Appendix*, Fig. S12).

Importance of Melted Silica Glass. Lechatelierite is only known to occur as a product of impact events, nuclear detonations, and lightning strikes (15). We observed it in spherules and SLOs from Abu Hureyra, Blackville, and Melrose (Fig. 5), suggesting an origin by one of those causes. Lechatelierite is found in material from Meteor Crater (16), Haughton Crater, the Australasian tektite field (17), Dakhleh Oasis (18), and the Libyan Desert Glass Field (17), having been produced from whole-rock melting of quartzite, sandstones, quartz-rich igneous and metamorphic rocks, and/or loess-like materials. The consensus is that melting begins above 1,700 °C and proceeds to temperatures $>2,200$ °C, the boiling point of quartz, within a time span of a few seconds depending on the magnitude of the event (26, 27). These temperatures restrict potential formation processes, because these are far higher than peak temperatures observed in magmatic

eruptions of $<1,300$ °C (28), wildfires at $<1,454$ °C (29), fired soils at $<1,500$ °C (30), glassy slag from natural biomass combustion at $<1,290$ °C (31), and coal seam fires at $<1,650$ °C (31).

Lechatelierite is also common in high-temperature, lightning-produced fulgurites, of which there are two types (for detailed discussion, see *SI Appendix*). First, subsurface fulgurites are glassy tube-like objects (usually <2 cm in diameter) formed from melted sediment at $>2,300$ °C. Second, exogenic fulgurites include vesicular glassy spherules, droplets, and teardrops (usually <5 cm in diameter) that are only rarely ejected during the formation of subsurface fulgurites. Both types closely resemble melted material from cosmic impact events and nuclear airbursts, but there are recognizable differences: (i) no collisions (fulgurites show no high-velocity collisional damage by other particles, unlike YDB SLOs and trinitite); (ii) different ultrastructure (subsurface fulgurites are tube-like, and broken pieces typically have highly reflective inner surfaces with sand-coated exterior surfaces, an ultrastructure unlike that of any known YDB SLO); (iii) lateral distribution (exogenic fulgurites are typically found <1 m from the point of a lightning strike, whereas the known lateral distribution of impact-related SLOs is 4.5 m at Abu Hureyra, 10 m at Blackville, and 28 m at Melrose); and (iv) rarity (at 18 sites investigated, some spanning $>16,000$ years, we did not observe any fulgurites or fragments in any stratum). Pigati et al. (14) confirmed the presence of YDB spherules and iridium at Murray Springs, AZ, but proposed that cosmic, volcanic, and impact melt products have been concentrated over time beneath black mats and in deflational basins, such as are present at eight of our sites that have wetland-derived black mats. In this study, we did not observe any fulguritic glass or YDB SLOs beneath any wetland black mats, contradicting Pigati et al., who propose that they should concentrate such materials. We further note that the enrichment in spherules reported by Pigati et al. at four non-YDB sites in Chile are most likely caused by volcanism, because their collection sites are located 20–80 km downslope from 22 major active volcanoes in the Andes (14). That group performed no

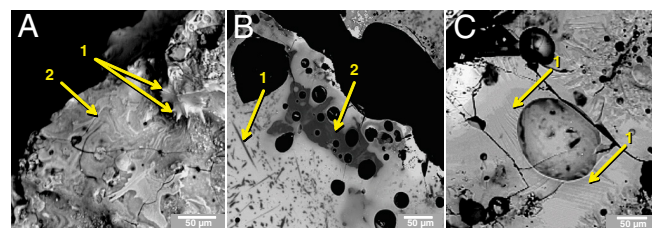


Fig. 5. SEM-BSE images of high-temperature SLOs with lechatelierite. (A) Abu Hureyra: portion of a dense 4-mm chunk of lechatelierite. Arrows identify tacky, viscous protrusions (no. 1) and high-temperature flow lines or schlieren (no. 2). (B) Blackville: Polished section of SLO displays vesicles, needle-like mullite quench crystals (no. 1), and dark grey lechatelierite (no. 2). (C) Melrose: Polished section of a teardrop displays vesicles and lechatelierite with numerous schlieren (no. 1).

SEM or EDS analyses to determine whether their spherules are volcanic, cosmic, or impact-related, as stipulated by Firestone et al. (1) and Israde-Alcántara et al. (4)

Pre-Industrial anthropogenic activities can be eliminated as a source of lechatelierite because temperatures are too low to melt pure SiO₂ at >1,700 °C. For example, pottery-making began at approximately 14 ka but maximum temperatures were <1,050 °C (31); glass-making at 5 ka was at <1,100 °C (32) and copper-smelting at 7 ka was at <1,100 °C (32). Humans have only been able to produce temperatures >1,700 °C since the early 20th century in electric-arc furnaces. Only a cosmic impact event could plausibly have produced the lechatelierite contained in deeply buried sediments that are 12.9 kiloyears (kyrs) old.

SiO₂ glass exhibits very high viscosity even at melt temperatures of >1,700 °C, and flow textures are thus difficult to produce until temperatures rise much higher. For example, Wasson and Moore (33) noted the morphological similarity between Australasian tektites and LDG, and therefore proposed the formation of LDG by a cosmic aerial burst. They calculated that for low-viscosity flow of SiO₂ to have occurred in Australasian tektites and LDG samples, temperatures of 2,500–2,700 °C were required. For tektites with lower SiO₂ content, requisite minimum temperatures for flow production may have been closer to 2,100–2,200 °C. Lechatelierite may form schlieren in mixed glasses (27) when viscosity is low enough. Such flow bands are observed in SLOs from Abu Hureyra and Melrose (Fig. 5) and if the model of Wasson and Moore (33) is correct, then an airburst/impact at the YDB produced high-temperature melting followed by rapid quenching (15). Extreme temperatures in impact materials are corroborated by the identification of frothy lechatelierite in Muong Nong tektites reported by Walter (34), who proposed that some lechatelierite cores displayed those features because of the boiling of quartz at 2,200 °C. We surveyed several hundred such lechatelierite grains in 18 Muong Nong tektites and found similar evidence of boiling; most samples retained outlines of the precursor quartz grains (*SI Appendix, Fig. S13*).

To summarize the evidence, only two natural processes can form lechatelierite: cosmic impacts and lightning strikes. Based on the evidence, we conclude that YDB glasses are not fulgurites. Their most plausible origin is by cosmic impact.

Collision and Accretion Features. Evidence for interparticle collisions is observed in YDB samples from Abu Hureyra, Blackville, and Melrose. These highly diagnostic features occur within an impact plume when melt droplets, rock particles, dust, and partially melted debris collide at widely differing relative velocities. Such features are only known to occur during high-energy atomic detonations and cosmic impacts, and, because differential velocities are too low^{††}, have never been reported to have been caused by volcanism, lightning, or anthropogenic processes. High-speed collisions can be either constructive, whereby partially molten, plastic spherules grow by the accretion of smaller melt droplets (35), or destructive, whereby collisions result in either annihilation of spherules or surface scarring, leaving small craters (36). In destructive collisions, small objects commonly display three types of collisions (36): (i) microcraters that display brittle fracturing; (ii) lower-velocity craters that are often elongated, along with very low-impact “furrows” resulting from oblique impacts (Fig. 6); and (iii) penetrating collisions between particles that result in melting and deformational damage (Fig. 7). Such destructive damage can occur between impactors of the same or different sizes and compositions, such as carbon impactors colliding with Fe-rich spherules (*SI Appendix, Fig. S14*).

Collisions become constructive, or accretionary, at very low velocities and show characteristics ranging from disrupted projec-

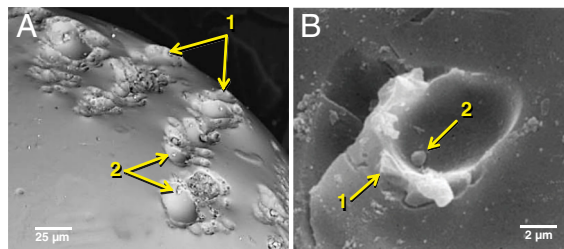


Fig. 6. SEM-BSE images of impact pitting. (A) Melrose: cluster of oblique impacts on a SLO that produced raised rims (no. 1). Tiny spherules formed in most impact pits together with irregularly shaped impact debris (no. 2). (B) Australasian tektite: Oblique impact produced a raised rim (no. 1). A tiny spherule is in the crater bottom (no. 2) (36).

tiles to partial burial and/or flattening of projectiles on the accreting host (Fig. 8 *A* and *B*). The least energetic accretions are marked by gentle welding together of tacky projectiles. Accretionary impacts are the most common type observed in 36 glassy impactites from Meteor Crater and in YDB spherules and SLOs (examples in Fig. 9). Other types of accretion, such as irregular melt drapings and filament splatter (37), are common on YDB objects and melt products from Meteor Crater (Fig. 9*D*). Additional examples of collisions and splash forms are shown in *SI Appendix, Fig. S15*. This collective evidence is too energetic to be consistent with any known terrestrial mechanism and is unique to high-energy cosmic impact events.

YDB Objects by Site. Blackville, South Carolina. High-temperature melt products consisting of SLOs (420–2,700 μm) and glassy spherules (15–1,940 μm) were collected at a depth of 1.75–1.9 m. SLOs range from small, angular, glassy, shard-like particles to large clumps of highly vesiculated glasses, and may contain pockets of partially melted sand, clay, mineral fragments, and carbonaceous matter. Spherules range from solid to vesicular, and some are hollow with thin to thick walls, and the assemblage also includes welded glassy spherules, thermally processed clay clasts, and partially melted clays.

Spherules show a considerable variation in composition and oxygen fugacity, ranging from highly reduced, Al—Si-rich glasses to dendritic, oxidized iron oxide masses. One Blackville spherule (Fig. 10*A*) is composed of Al₂O₃-rich glasses set with lechatelierite, suessite, spheres of native Fe, and quench crystallites of corundum and 2:1 mullite, one of two stoichiometric forms of mullite (2Al₂O₃:SiO₂, or 2:1 mullite; and 3Al₂O₃:2SiO₂, or 3:2 mullite). This spherule is an example of the most reduced melt with oxygen fugacity (*f*O₂) along the IW (iron—wüstite) buffer. Other highly oxidized objects formed along the H or magnetite—hematite buffer. For example, one hollow spherule contains 38% by volume of dendritic aluminous hematite (*SI Appendix, Fig. S16*) with minor amounts of unidentified iron

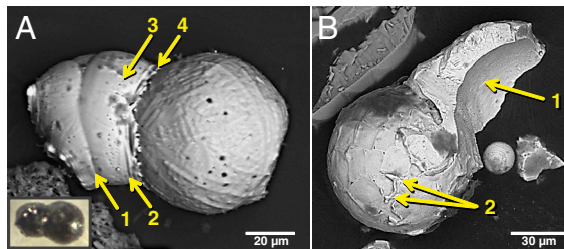


Fig. 7. SEM-BSE images of collisional spherules. (A) Lake Cuitzeo, Mexico: collision of two spherules at approximately tens of m/s; left spherule underwent plastic compaction to form compression rings (nos. 1 and 2), a line of gas vesicles (no. 3), and a splash apron (no. 4). (B) Kimbel Bay: Collision of two spherules destroyed one spherule (no. 1) and formed a splash apron on the other (no. 2). This destructive collision suggests high differential velocities of tens to hundreds of m/s.

^{††}Buchner E, Schmeider M, Strasser A, Krochert L, Impacts on spherules, 40th Lunar and Planetary Science Conference. March 26, 2009, abstr 1017.

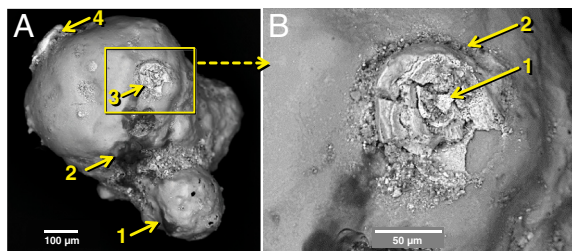


Fig. 8. SEM-BSE images of accretionary features. (A) Melrose: lumpy spherule with a subrounded accretion (no. 1), a dark carbon accretion (no. 2), and two hollow, magnetic spherules flattened by impact (nos. 3 and 4). (B) Melrose: enlargement of box in A, displaying fragmented impacting magnetic spherule (no. 1) forming a debris ring (no. 2) that partially fused with the aluminosilicate host spherule.

oxides set in Fe-rich glass with no other crystallites. One Blackville SLO is composed of high Al_2O_3 - SiO_2 glass with dendritic magnetite crystals and vesicles lined with vapor-deposited magnetite (*SI Appendix, Fig. S17*). In addition to crystallizing from the glass melt, magnetite also crystallized contemporaneously with glassy carbon. These latter samples represent the most oxidized of all objects, having formed along the H or magnetite-hematite buffer, displaying 10- to 20- μm diameter cohenite (Fe_3C) spheres with inclusions of Fe phosphide (Fe_2P - Fe_3P) containing up to 1.10 wt% Ni and 0.78 wt% Co. These occur in the reduced zones of spherules and SLOs, some within tens of μm of highly oxidized Al-hematite. These large variations in composition and oxygen fugacity over short distances, which are also found in Trinity SLOs and spherules, are the result of local temperature and physico-chemical heterogeneities in the impact plume. They are consistent with cosmic impacts, but are inconsistent with geological and anthropogenic mechanisms.

Spherules and SLOs from Blackville are mostly aluminosilicate glasses, as shown in the ternary phase diagrams in *SI Appendix, Fig. S9*, and most are depleted in $\text{K}_2\text{O} + \text{Na}_2\text{O}$, which may reflect

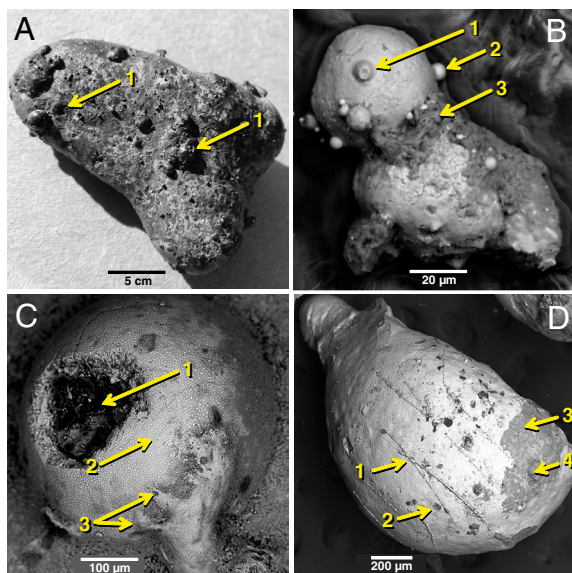


Fig. 9. Accretion textures. (A) Meteor Crater: glassy impactite with multiple accretionary objects deformed by collisional impact (no. 1). (B) Talega site: cluster of large quenched spherules with smaller partially buried spherules (no. 1), accretion spherules (no. 2), and accreted carbonaceous matter (no. 3). (C) Meteor Crater: accretion spherule on larger host with impact pit lined with carbon (no. 1), quenched iron oxide surface crystals (light dots at no. 2), and melt draping (no. 3). (D) Melrose: YDB teardrop with a quench crust of aluminosilicate glass and a subcrust interior of SiO_2 and Al-rich glasses, displaying melt drappings (no. 1), microcraters (no. 2), mullite crystals (no. 3), and accretion spherules (no. 4).

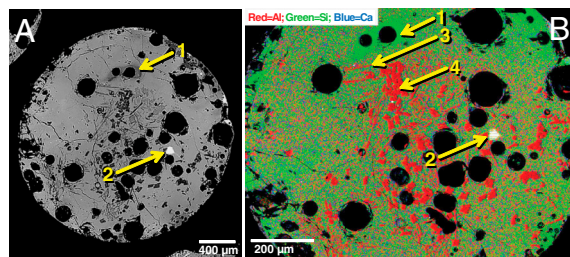


Fig. 10. SEM-BSE images of Blackville spherule. (A) Sectioned spherule composed of high-temperature, vesiculated aluminosilicate glass and displaying lechatelierite (no. 1) and reduced-Fe spherules (no. 2). (B) False-colored enlargement of same spherule displaying lechatelierite (green, no. 1) and reduced-Fe spherules (white, no. 2) with needle-like mullite quench crystals (red, no. 3) and corundum quench crystals (red, no. 4).

high melting temperatures and concomitant loss of volatile elements that increases the refractoriness of the melts. For most spherules and SLOs, quench crystallites are limited to corundum and mullite, although a few have the Fe-Al spinel, hercynite. These phases, together with glass compositions, limit the compositional field to one with maximum crystallization temperatures ranging from approximately 1,700–2,050 $^{\circ}\text{C}$. The spherule in Fig. 10A is less alumina-rich, but contains suessite (Fe_3Si), which indicates a crystallization temperature of 2,000–2,300 $^{\circ}\text{C}$ (13, 38).

Observations of clay-melt interfaces with mullite or corundum-rich inclusions indicate that the melt glasses are derived from materials enriched in kaolinite with smaller amounts of quartz and iron oxides. Partially melted clay discontinuously coated the surfaces of a few SLOs, after which mullite needles grew across the clay-glass interface. The melt interface also has quench crystals of magnetite set in Fe-poor and Fe-rich glasses (*SI Appendix, Fig. S18*). SLOs also contain carbon-enriched black clay clasts displaying a considerable range of thermal decomposition in concert with increased vesiculation and vitrification of the clay host. The interfaces between mullite-rich glass and thermally decomposed black clay clasts are frequently decorated with suessite spherules.

Abu Hureyra site, Syria. The YDB layer yielded abundant magnetic and glass spherules and SLOs containing lechatelierite intermixed with CaO-rich glasses. Younger layers contain few or none of those markers (*SI Appendix, Table S3*). The SLOs are large, ranging in size up to 5.5 mm, and are highly vesiculated (*SI Appendix, Fig. S19*); some are hollow and some form accretionary groups of two or more objects. They are compositionally and morphologically similar to melt glasses from Meteor Crater, which, like Abu Hureyra, is located in Ca-rich terrain (*SI Appendix, Fig. S21*). YDB magnetic spherules are smaller than at most sites (20–50 μm). Lechatelierite is abundant in SLOs and exhibits many forms, including sand-size grains and fibrous textured objects with intercalated high-CaO glasses (Fig. 11). This fibrous morphology, which has been observed in material from Meteor Crater and Houghton Crater (*SI Appendix,*

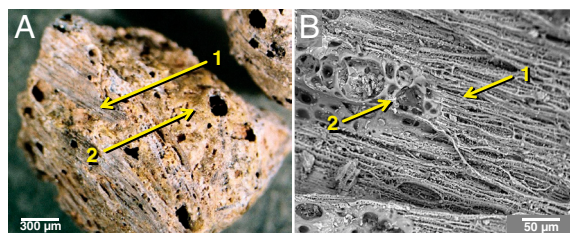


Fig. 11. (A) Abu Hureyra: SLO (2 mm wide) with grey tabular lechatelierite grains (no. 1) surrounded by tan CaO-rich melt (no. 2). (B) SEM-BSE image showing fibrous lechatelierite (no. 1) and bubbled CaO-rich melt (no. 2).

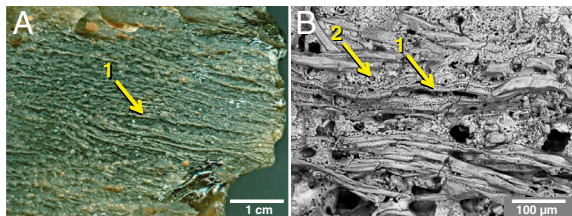


Fig. 12. (A) Libyan Desert Glass (7 cm wide) displaying tubular glassy texture (no. 1). (B) Abu Hureyra: lechatelierite tubes (no. 1) disturbed by chaotic plastic flow and embedded in a vesicular, CaO-rich matrix (no. 2).

(Fig. S22), exhibits highly porous and vesiculated lechatelierite textures, especially along planes of weakness that formed during the shock compression and release stage. During impact, the SiO_2 melted at very high post-shock temperatures ($>2,200^\circ\text{C}$), produced taffy-like stringers as the shocked rock pulled apart during decompression, and formed many tiny vesicles from vapor outgassing. We also observed distorted layers of hollow vesiculated silica glass tube-like features, similar to some LDG samples (Fig. 12), which are attributed to relic sedimentary bedding structures in the sandstone precursor (39). The Abu Hureyra tubular textures may be relic structures of thin-bedded chert that occurs within the regional chalk deposits. These clusters of aligned micron-sized tubes are morphologically unlike single, centimeter-sized fulgurites, composed of melted glass tubes encased in unmelted sand. The Abu Hureyra tubes are fully melted with no sediment coating, consistent with having formed aerially, rather than below ground.

At Abu Hureyra, glass spherules have compositions comparable to associated SLOs (SI Appendix, Table S4) and show accretion and collision features similar to those from other YDB sites. For example, low-velocity elliptical impact pits were observed that formed by low-angle collisions during aerodynamic rotation of a spherule (Fig. 13A). The shape and low relief of the rims imply that the spherule was partially molten during impact. It appears that these objects were splattered with melt drapings while rotating within a debris cloud. Linear, subparallel, high- SiO_2 melt strands (94 wt% SiO_2) are mostly embedded within the high-CaO glass host, but some display raised relief on the host surface, thus implying that both were molten. An alternative explanation is that the strands are melt relics of precursor silica similar to fibrous lechatelierite (Fig. 11).

Melrose site, Pennsylvania. As with other sites, the Melrose site displays exotic YDB carbon phases, magnetic and glassy spherules, and coarse-grained SLOs up to 4 mm in size. The SLOs exhibit accretion and collision features consistent with flash melting and interactions within a debris cloud. Teardrop shapes are more common at Melrose than at other sites, and one typical teardrop (Fig. 14 A and B) displays high-temperature melt glass with mullite quench crystals on the glassy crust and with corundum in the

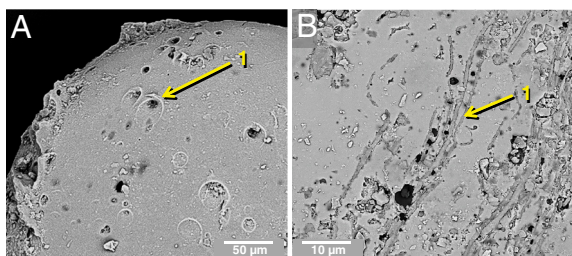


Fig. 13. Abu Hureyra: (A) SLO with low-angle impact craters (no. 1); half-formed rims show highest relief in direction of impacts and/or are counter to rotation of spherule. (B) Enlargement showing SiO_2 glass strands (no. 1) on and in surface.

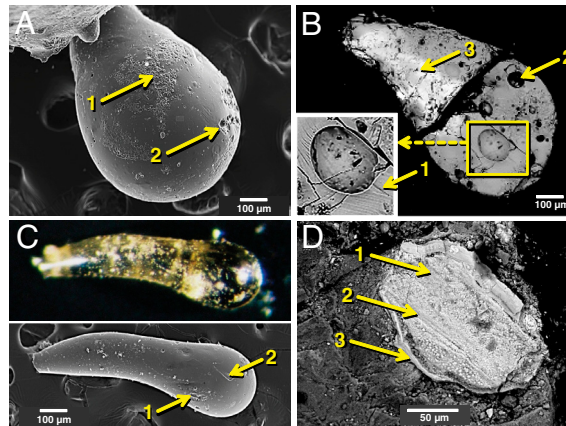


Fig. 14. Melrose. (A) Teardrop with aluminosilicate surface glass with mullite quench crystals (no. 1) and impact pits (no. 2). (B) Sectioned slide of A showing lechatelierite flow lines emanating from the nose (Inset, no. 1), vesicles (no. 2), and patches of quenched corundum and mullite crystals. The bright area (no. 3) is area with 30 wt% FeO compared with 15 wt% in darker grey areas. (C) Reflected light photomicrograph of C teardrop (Top) and SEM-BSE image (Bottom) of teardrop that is compositionally homogeneous to A; displays microcraters (no. 1) and flow marks (no. 2). (D) Melted magnetite (no. 1) embedded in glass-like carbon. The magnetite interior is composed of tiny droplets atop massive magnetite melt displaying flow lines (no. 2). The rapidly quenched rim with flow lines appears splash formed (no. 3).

interior. This teardrop is highly vesiculated and compositionally heterogeneous. FeO ranges from 15–30 wt%, SiO_2 from 40–48 wt%, and Al_2O_3 from 21–31 wt%. Longitudinally oriented flow lines suggest the teardrop was molten during flight. These teardrops (Fig. 14 A–C) are interpreted to have fallen where excavated because they are too fragile to have been transported or reworked by alluvial or glacial processes. If an airburst/impact created them, then these fragile materials suggest that the event occurred near the sampling site.

Other unusual objects from the Melrose site are high-temperature aluminosilicate spherules with partially melted accretion rims, reported for Melrose in Wu (13), displaying melting from the inside outward, in contrast to cosmic ablation spherules that melt from the outside inward. This characteristic was also observed in trinitite melt beads that have lechatelierite grains within the interior bulk glasses and partially melted to unmelted quartz grains embedded in the surfaces (22), suggesting that the quartz grains accreted within the hot plume. The heterogeneity of Melrose spherules, in combination with flow-oriented suessite and FeO droplets, strongly suggests that the molten host spherules accreted a coating of bulk sediment while rotating within the impact plume.

The minimum temperature required to melt typical bulk sediment is approximately $1,200^\circ\text{C}$; however, for mullite and corundum solidus phases, the minimum temperature is $>1,800^\circ$. The presence of suessite (Fe_3Si) and reduced native Fe implies a minimum temperature of $>2,000^\circ\text{C}$, the requisite temperature to promote liquid flow in aluminosilicate glass. Another high-temperature indicator is the presence of embedded, melted magnetite (melting point, $1,550^\circ\text{C}$) (Fig. 14D), which is common in many SLOs and occurs as splash clumps on spherules at Melrose (SI Appendix, Fig. S23). In addition, lechatelierite is common in SLOs and glass spherules from Melrose; the minimum temperature for producing schlieren is $>2,000^\circ\text{C}$.

Trinity nuclear site, New Mexico. YDB objects are posited to have resulted from a cosmic airburst, similar to ones that produced Australasian tektites, Libyan Desert Glass, and Dakhleh Glass. Melted material from these sites is similar to melt glass from an atomic detonation, even though, because of radioactive materials, the means of surface heating is somewhat more complex

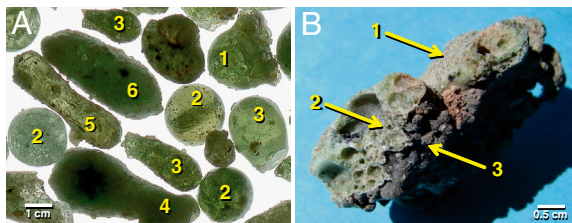


Fig. 15. Trinity detonation. (A) Assortment of backlit, translucent trinitite shapes: accretionary (no. 1), spherulitic (no. 2), broken teardrop (no. 3), bottle-shaped (no. 4), dumbbell (no. 5), elongated or oval (no. 6). (B) Edge-on view of a pancake trinitite with smooth top (no. 1), vesiculated interior (no. 2), and dark bottom (no. 3) composed of partially fused rounded trinitite objects incorporated with surface sediment.

(SI Appendix). To evaluate a possible connection, we analyzed material from the Alamogordo Bombing Range, where the world's first atomic bomb was detonated in 1945. Surface material at Trinity ground zero is mostly arkosic sand, composed of quartz, feldspar, muscovite, actinolite, and iron oxides. The detonation created a shallow crater (1.4 m deep and 80 m in diameter) and melted surface sediments into small glass beads, teardrops, and dumbbell-shaped glasses that were ejected hundreds of meters from ground zero (Fig. 15A). These objects rained onto the surface as molten droplets and rapidly congealed into pancake-like glass puddles (SI Appendix, Fig. S24). The top surface of this ejected trinitite is bright to pale grey-green and mostly smooth; the interior typically is heavily vesiculated (Fig. 17B). Some of the glassy melt was transported in the rising cloud of hot gases and dispersed as distal ejecta.

Temperatures at the interface between surface minerals and the puddled, molten trinitite can be estimated from the melting behavior of quartz grains and K-feldspar that adhered to the molten glass upon impact with the ground (SI Appendix, Fig. S22). Some quartz grains were only partly melted, whereas most other quartz was transformed into lechatelierite (26). Similarly, the K-feldspar experienced partial to complete melting. These observations set the temperature range from 1,250 °C (complete melting of K-feldspar) to >1,730 °C (onset of quartz melting). Trinitite samples exhibit the same high-temperature features as observed in materials from hard impacts, known airbursts, and the YDB layer. These include production of lechatelierite from quartz ($T = 1,730\text{--}2,200\text{ °C}$), melting of magnetite and ilmenite to form quench textures ($T \geq 1,550\text{ °C}$), reduction of Fe to form native Fe spherules, and extensive flow features in bulk melts and lechatelierite grains (Fig. 16). The presence of quenched magnetite and native iron spherules in trinitite strongly suggests extreme oxygen fugacity conditions over very short distances (Fig. 17B); similar objects were observed in Blackville SLOs (Fig. 10A). Other features common to trinitite and YDB objects include accretion of spherules/beads on larger objects, impact microcratering, and melt draping (Figs. 16 and 17).

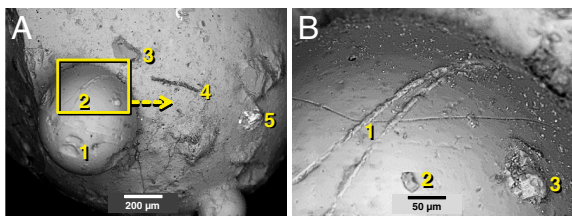


Fig. 16. Trinitite produced by debris cloud interactions. (A) Trinitite spherule showing accreted glass bead with impact pits (no. 1); melt drappings (no. 2); and embedded partially melted quartz grain (no. 3), carbon filament (no. 4), and melted magnetite grain (no. 5). (B) Enlarged image of box in A showing melt drappings (no. 1), and embedded partially melted quartz grain (no. 2) and melted magnetite grains (no. 3). See Fig. 9D for similar YDB melt drappings.

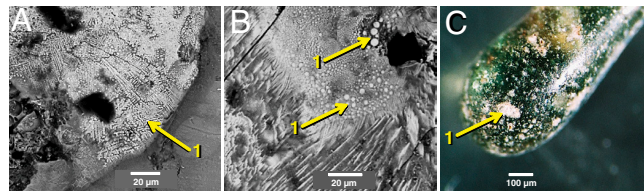


Fig. 17. Trinity: characteristics of high-temperature melting. (A) SEM-BSE image of bead in trinitite that is mostly quenched, dendritic magnetite (no. 1). (B) Melt beads of native Fe in etched glass (no. 1). (C) Heavily pitted head of a trinitite teardrop (no. 1) resulting from collisions in the debris cloud.

The Trinity nuclear event, a high-energy airburst, produced a wide range of melt products that are morphologically indistinguishable from YDB objects that are inferred to have formed during a high-energy airburst (SI Appendix, Table S1). In addition, those materials are morphologically indistinguishable from melt products from other proposed cosmic airbursts, including Australasian tektites, Dakhleh Glass, and Tunguska spherules and glass. All this suggests similar formation mechanisms for the melt materials observed in of these high-energy events.

Methods

YDB objects were extracted by 15 individuals at 12 different institutions, using a detailed protocol described in Firestone et al. (1) and Israde-Alcántara et al. (4). Using a neodymium magnet (5.15 × 2.5 × 1.3 cm; grade N52 NdFeB; magnetization vector along 2.5-cm face; surface field density = 0.4 T; pull force = 428 N) tightly wrapped in a 4-mil plastic bag, the magnetic grain fraction (dominantly magnetite) was extracted from slurries of 300–500 g bulk sediment and then dried. Next, the magnetic fraction was sorted into multiple size fractions using a stack of ASTM sieves ranging from 850–38 μm. Aliquots of each size fraction were examined using a 300× reflected light microscope to identify candidate spherules and to acquire photomicrographs (Fig. 1), after which candidate spherules were manually selected, tallied, and transferred to SEM mounts. SEM-EDS analysis of the candidate spherules enabled identification of spherules formed through cosmic impact compared with terrestrial grains of detrital and framboidal origin. From the magnetic fractions, SLO candidates >250 μm were identified and separated manually using a light microscope from dry-sieved aliquots and weighed to provide abundance estimates. Twelve researchers at 11 different universities acquired SEM images and obtained >410 analyses. Compositions of YDB objects were determined using standard procedures for SEM-EDS, electron microprobe, INAA, and PGAA.

Conclusions

Abundance peaks in SLOs were observed in the YDB layer at three dated sites at the onset of the YD cooling episode (12.9 ka). Two are in North America and one is in the Middle East, extending the existence of YDB proxies into Asia. SLO peaks are coincident with peaks in glassy and Fe-rich spherules and are coeval with YDB spherule peaks at 15 other sites across three continents. In addition, independent researchers working at one well-dated site in North America (8) and one in South America (10–12) have reported YDB melt glass that is similar to these SLOs. YDB objects have now been observed in a total of eight countries on four continents separated by up to 12,000 km with no known limit in extent. The following lines of evidence support a cosmic impact origin for these materials.

Geochemistry. Our research demonstrates that YDB spherules and SLOs have compositions similar to known high-temperature, impact-produced material, including tektites and ejecta. In addition, YDB objects are indistinguishable from high-temperature melt products formed in the Trinity atomic explosion. Furthermore, bulk compositions of YDB objects are inconsistent with known cosmic, anthropogenic, authigenic, and volcanic materials, whereas they are consistent with intense heating, mixing, and quenching of local terrestrial materials (mud, silt, clay, shale).

Morphology. Dendritic texturing of Fe-rich spherules and some SLOs resulted from rapid quenching of molten material. Requisite temperatures eliminate terrestrial explanations for the 12.9-kyr-old material (e.g., frambooids and detrital magnetite), which show no evidence of melting. The age, geochemistry, and morphology of SLOs are similar across two continents, consistent with the hypothesis that the SLOs formed during a cosmic impact event involving multiple impactors across a wide area of the Earth.

Lechatelierite and Schlieren. Melting of SLOs, some of which are >80% SiO₂ with pure SiO₂ inclusions, requires temperatures from 1,700–2,200 °C to produce the distinctive flow-melt bands. These features are only consistent with a cosmic impact event and preclude all known terrestrial processes, including volcanism, bacterial activity, authigenesis, contact metamorphism, wildfires, and coal seam fires. Depths of burial to 14 m eliminate modern anthropogenic activities as potential sources, and the extremely high melting temperatures of up to 2,200 °C preclude anthropogenic activities (e.g., pottery-making, glass-making, and metal-smelting) by the contemporary cultures.

Microcratering. The YDB objects display evidence of microcratering and destructive collisions, which, because of the high initial and differential velocities required, form only during cosmic impact events and nuclear explosions. Such features do not result from anthropogenesis or volcanism.

Summary. Our observations indicate that YDB objects are similar to material produced in nuclear airbursts, impact crater plumes, and cosmic airbursts, and strongly support the hypothesis of multiple cosmic airburst/impacts at 12.9 ka. Data presented here require that thermal radiation from air shocks was sufficient to melt surface sediments at temperatures up to or greater than the boiling point of quartz (2,200 °C). For impacting cosmic fragments, larger melt masses tend to be produced by impactors with greater mass, velocity, and/or closeness to the surface. Of the 18 investigated sites, only Abu Hureyra, Blackville, and Melrose display large melt masses of SLOs, and this observation suggests that each of these sites was near the center of a high-energy airburst/impact. Because these three sites in North America and the Middle East are separated by 1,000–10,000 km, we propose that there were three or more major impact/airburst epicenters for the YDB impact event. If so, the much higher concentration of SLOs at Abu Hureyra suggests that the effects on that settlement and its inhabitants would have been severe.

ACKNOWLEDGMENTS. We thank Malcolm LeCompte, Scott Harris, Yvonne Malinowski, Paula Zitzelberger, and Lawrence Edge for providing crucial samples, data, and other assistance; and Anthony Irving, Richard Grieve, and two anonymous reviewers for useful reviews and comments on this paper. This research was supported in part by US Department of Energy Contract DE-AC02-05CH11231 and US National Science Foundation Grant 9986999 (to R.B.F.); US National Science Foundation Grants ATM-0713769 and OCE-0825322, Marine Geology and Geophysics (to J.P.K.); US National Science Foundation Grant OCE-0244201 (to D.J.K.); and US National Science Foundation Grant EAR-0609609, Geophysics (to G.K.).

1. Firestone RB, et al. (2007) Evidence for an extraterrestrial impact 12,900 years ago that contributed to the megafaunal extinctions and the Younger Dryas cooling. *Proc Natl Acad Sci USA* 104:16016–16021.
2. Haynes CV, Jr (2008) Younger Dryas “black mats” and the Rancholabrean termination in North America. *Proc Natl Acad Sci USA* 105:6520–6525.
3. Kennett DJ, et al. (2009) Shock-synthesized hexagonal diamonds in Younger Dryas boundary sediments. *Proc Natl Acad Sci USA* 106:12623–12628.
4. Israde-Alcántara I, et al. (2012) Evidence from central Mexico supporting the Younger Dryas extraterrestrial impact hypothesis. *Proc Natl Acad Sci USA* 109: E738–E747.
5. Melott AL, Thomas BC, Dreschhoff G, Johnson CK (2010) Cometary airbursts and atmospheric chemistry: Tunguska and a candidate Younger Dryas event. *Geology* 38:355–358.
6. Surovell TA, et al. (2009) An independent evaluation of the Younger Dryas extraterrestrial impact hypothesis. *Proc Natl Acad Sci USA* 104:18155–18158.
7. Pinter N, et al. (2011) The Younger Dryas impact hypothesis: A requiem. *Earth-Sci Rev* 106:247–264.
8. Fayek M, Anovitz LM, Allard LF, Hull S (2012) Frambooidal iron oxide: Chondrite-like material from the black mat, Murray Springs, Arizona. *Earth Planet Sci Lett* 319–320:251–258.
9. Haynes CV, Jr, et al. (2010) The Murray Springs Clovis site, Pleistocene extinction, and the question of extraterrestrial impact. *Proc Natl Acad Sci USA* 107:4010–4015.
10. Mahaney WC, et al. (2010) Evidence from the northwestern Venezuelan Andes for extraterrestrial impact: The black mat enigma. *Geomorphology* 116:48–57.
11. Mahaney WC, et al. (2011) Fired glaciofluvial sediment in the northwestern Andes: Biotic aspects of the black mat. *Sediment Geol* 237:73–83.
12. Mahaney WC, Krinsley D (2012) Extreme heating events and effects in the natural environment: Implications for environmental geomorphology. *Geomorphology* 139–140:348–359.
13. Wu Y (2011) Origin and provenance of magnetic spherules at the Younger Dryas boundary. Thesis (Dartmouth College, Hanover, NH).
14. Pigati JS, et al. (2012) Accumulation of “impact markers” in desert wetlands and implications for the Younger Dryas impact hypothesis. *Proc Natl Acad Sci USA* 109:7208–7212.
15. French BM (1998) *Traces of Catastrophe*. LPI Contribution No. 954 (LPI, Houston), pp 102–103.
16. Chao ETC (1967) Shock effects in certain rock forming minerals. *Science* 156:192–202.
17. Wasson J (2003) Large aerial bursts: An important class of terrestrial accretionary events. *Astrobiology* 3:163–179.
18. Osinski GR, et al. (2008) The Dakhleh Glass: Product of an impact airburst or cratering event in the Western Desert of Egypt? *Meteorit Planet Sci* 43:2089–2107.
19. Kirova OA, Zaslavskaya NI (1966) Data characterizing the dispersed matter as recovered from the area of fall of the Tunguska meteorite. *Meteoritika* 27:119–127.
20. Hermes RE, Strickfaden WB (2005) A new look at trinitite. *J Nucl Weap* 2:2–7.
21. Moore AMT, Hillman GC, Legge AJ (2000) *Village on the Euphrates* (Oxford University Press, New York).
22. Eby N, Hermes R, Charnley N, Smoliga JA (2010) Trinitite: The atomic rock. *Geol Today* 26:181–186.
23. Taylor S, Lever JH, Harvey RP (2000) Numbers, types, and compositions of an unbiased collection of cosmic spherules. *Meteorit Planet Sci* 35:651–666.
24. Doyle LJ, Hopkins TL, Betzer PR (1976) Black magnetic spherule fallout in the eastern Gulf of Mexico. *Science* 194:1157–1159.
25. Glass BP, Senftle FE, Muenow DW, Aggrey KE, Thorpe AN (1987) Atomic bomb glass beads: Tektite and microtektite analogs. *Proceedings of the Second International Conference on Natural Glasses*, ed J Konta (Charles University, Prague), pp 361–369.
26. Grieve RAF, Pillington M (1996) The significance of terrestrial impact craters. *AGSO J Aust Geol Geophys* 16:399–420.
27. Stöffler D, Langenhorst F (1994) Shock metamorphism of quartz in nature and experiments: I. Basic observations and theory. *Meteorit Planet Sci* 31:6–35.
28. Rutherford MJ, Devine JD, III (2008) Magmatic conditions and processes in the storage zone of the 2004–2006 Mount St. Helens dacite. *US Geological Survey Professional Paper* 1750.
29. Philpot CW (1965) *Temperatures in a Large Natural-Fuel Fire* (US Forestry Service, Pacific Southwest Forest and Range Experimental Station, Berkeley), Research Note PSW-90.
30. Gimeno-Garcia E, Andreu E, Rubio JL (2004) Spatial patterns of soil temperatures during experimental fires. *Geoderma* 118:17–38.
31. Thy P (1995) Implications of prehistoric glassy biomass slag from east-central Botswana. *J Archaeol Sci* 22:629–637.
32. Beretta M (2009) *The Alchemy of Glass: Counterfeit, Imitation, and Transmutation in Ancient Glassmaking* (Science History Publications, Sagamore Beach).
33. Wasson JT, Moore K (1998) Possible formation of Libyan Desert Glass by a Tunguska-like aerial burst. *Meteorit Planet Sci* 33(Suppl):A163–A164.
34. Walter LS (1965) Coesite discovered in tektites. *Science* 147:1029–1032.
35. Kyte F, et al. (2010) Accretionary growth on impact spherules. *Meteorit Planet Sci* 45 (Suppl 5):A113–A113.
36. Prasad MS, Khedekar VD (2003) Impact microcrater morphology on Australasian microtektites. *Meteorit Planet Sci* 38:1351–1371.
37. Mirsa S, et al. (2010) Geochemical identification of impactor for Lonar Crater, India. *Meteorit Planet Sci* 44:1001–1018.
38. Rietmeijer FJM, et al. (2008) Origin and formation of iron silicide phases in the aerogel of the Stardust mission. *Meteorit Planet Sci* 43:121–134.
39. Longinelli A, et al. (2011) Delta ¹⁸O and chemical composition of Libyan Desert Glass, country rocks, and sands: New considerations on target material. *Meteorit Planet Sci* 46:218–227.
40. Winkler HGF (1979) *Petrogenesis of Metamorphic Rocks* (Springer, New York).
41. US Geological Survey (2001) (USGS, Reston). *Geochemistry of Soils in the US from the PLUTO Database* (USGS, Reston, VA).